Available online at www.sciencedirect.com
ScienceDirect
Journal of Catalysis 256 (2008) 15–23
JOURNAL OF CATALYSIS
www.elsevier.com/locate/jcat

In situ ATR-IR study of nitrite hydrogenation over Pd/Al_2O_3

Sune D. Ebbesen [1], Barbara L. Mojet, Leon Lefferts *

Catalytic Processes and Materials, Faculty of Science and Technology, Institute of Mechanics Processes and Control Twente (IMPACT) and MESA+ Institute for Nanotechnology, University of Twente – ME 357, P.O. Box 217, 7500 AE, Enschede, The Netherlands

Received 20 November 2007; revised 7 February 2008; accepted 15 February 2008

Available online 14 April 2008

Abstract

The mechanism of nitrite hydrogenation over a Pd/Al_2O_3 catalyst layer deposited on a ZnSe internal reflection element was investigated in water using attenuated total reflection infrared spectroscopy. Nitrite hydrogenates to $NO_{(ads)}$, $NH_{2(ads)}$, and NH_4^+ on the palladium surface. Hydrogenation of adsorbed NO on palladium results in the formation of a reaction product that is not infrared-active (most likely nitrogen), whereas no NH_4^+ is formed from $NO_{(ads)}$. NH_4^+ is formed solely from hydrogenation of the $NH_{2(ads)}$ intermediate. The present study clearly shows that formation of nitrogen and NH_4^+ proceeds via two separate pathways, based on which a revised reaction scheme is proposed.

Keywords: ATR-IR spectroscopy; Hydrogenation; Nitrite; Pd/Al_2O_3; Liquid phase; Water; Mechanism

1. Introduction

In recent years, much research has focused on technologies for groundwater treatment to remove nitrite and nitrate, due to increasing nitrite and nitrate concentrations in groundwater and increasingly strict regulation of drinking water quality [1]. Both biological and catalytic denitrification processes have potential for water purification [2]. The biological processes, however, have low reaction rates, making these processes insufficient for groundwater treatment [2]. The catalytic hydrogenation of nitrate and nitrite over noble metal catalysts, which was described for the first time in 1989 [3], is the most promising technique for nitrate and nitrite removal. To date, the catalytic hydrogenation of nitrite and nitrate for use in water purification has been examined extensively to develop efficient catalysts [3–14]; however, the mechanism of the nitrite hydrogenation over supported noble metal catalysts has not yet been resolved. Based on kinetic studies, adsorbed NO has been suggested as an intermediate [10]. Several authors have proposed a reaction scheme including adsorbed NO as the key intermediate for the catalytic hydrogenation of nitrate and nitrite over supported bimetallic catalysts, as schematically shown in Fig. 1 [11–14], although this scheme has not been supported by direct experimental evidence.

ATR-IR is ideally suited for studying molecular vibrations at the solid–liquid interface because the evanescent wave is restricted to the region near the interface, thereby minimizing the contribution from the liquid [15]. ATR-IR spectroscopic studies at the metal–liquid interface have started to receive attention only recently [16–23]. We have initiated a thorough investigation into the details of the catalytic hydrogenation of nitrite over platinum and palladium catalysts. We recently examined the adsorption of nitrite, hydroxylamine, and NH_4^+ on Pd/Al_2O_3 and Pt/Al_2O_3 by ATR-IR spectroscopy, to determine the type of adsorbates and possible intermediates during the hydrogenation of nitrite [24,25].

The objective of the present study is to gain insight into the mechanism of the heterogeneous hydrogenation of nitrite in water over Pd/Al_2O_3 by examining the surface intermediates during steady state as well as transient hydrogenation of nitrite over Pd/Al_2O_3 using ATR-IR spectroscopy.

* Corresponding author. Fax: +31 53 489 4683.
E-mail addresses: sune.ebbesen@risoe.dk (S.D. Ebbesen), l.lefferts@utwente.nl (L. Lefferts).
[1] Present address: Fuel Cells and Solid State Chemistry Department, Risø National Laboratory, Technical University of Denmark (DTU), Frederiksborgvej 399, DK-4000 Roskilde, Denmark.

0021-9517/$ – see front matter
doi:10.1016/j.jcat.2008.02.013

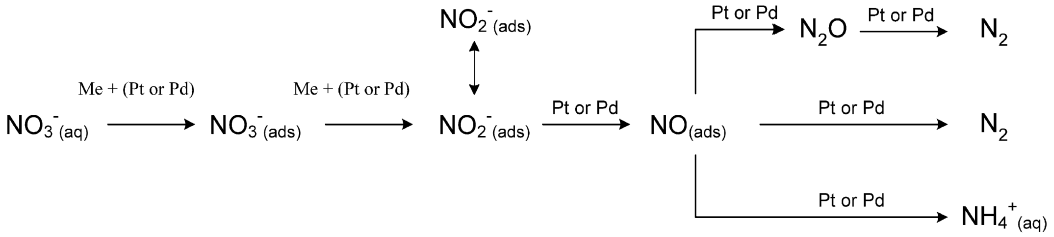

Fig. 1. Scheme of nitrate (and nitrite) hydrogenation over bimetallic platinum (Me/Pt) or palladium (Me/Pd) catalysts, after [11–14].

2. Experimental

2.1. Catalyst preparation and characterization

First, a Pd/Al_2O_3 powder catalyst was prepared and characterized. The catalyst powder was thereafter deposited on an ATR-IR ZnSe internal reflection element (IRE) and mounted in an *in situ* ATR-IR cell as described previously [17,23–25]. Details on catalyst preparation, characterization, and immobilization of the layer are available in those previous reports [17, 23–25]. In brief, a 5 wt% Pd/Al_2O_3 catalyst was prepared by adsorption of palladium acetylacetonate ($Pd(acac)_2$) (Alfa Aesar) on precalcined γ-Al_2O_3 powder. A suspension was prepared from Pd/Al_2O_3 in 50 mL of water; the pH was adjusted to 3.5 with nitric acid to stabilize the small alumina particles. The suspension was milled for 1 h in a ball mill (Fritsch Pulverisette) to obtain Al_2O_3 particles of a few nm in size. Subsequently, colloidal alumina (aluminium oxide, 20% in H_2O colloidal suspension, Alfa Aesar, particle size 5 nm) was added, and the catalyst layer was prepared on a ZnSe IRE by adding 1 mL of the catalyst/water suspension evenly on one side of the IRE. The suspension was allowed to evaporate overnight at room temperature. Subsequently, the catalyst layer/IRE was heated to 573 K for 2 h (at a heating rate of 1 K/min) in flowing argon to ensure removal of all NO_x species on the catalyst surface.

2.2. In situ ATR-IR spectroscopy

The water used in all ATR-IR experiments was ultra-pure Q2-water, prepared with a Millipore Milli-Q water treatment system (Amphotech Ltd.). Saturation of water with Ar (5.0, Praxair), or H_2 (5.0, Praxair), was performed at room temperature (294 K) with gas flow rates of 40 mL/min for a minimum of 2 h. Before saturation with H_2, air was removed by saturation with argon for at least 2 days. The concentrations of dissolved gases in water were calculated based on reported solubility data at room temperature and 1 atm gas pressure [26]. The Q2-water saturated with Ar (2.3×10^{-3} mol/L) or H_2 (4.1×10^{-4} mol/L) is designated as Ar/H_2O or H_2/H_2O in what follows.

A solution of $NO_{2(aq)}^-$ (4.3×10^{-4} mol/L) was prepared in Ar/H_2O from $NaNO_2$ (Merck). The pH was adjusted to 7.0 by adding NaOH (Merck); pH was measured using a pH meter (744 pH meter, Metrohm). For the continuous hydrogenation experiments, the nitrite solution was subsequently saturated with H_2/Ar mixtures; H_2 concentrations are indicated in the text.

ATR-IR spectra were recorded using a home-built stainless steel flow-through cell as described elsewhere [17,23–25]. The flow-through chamber was created by a spacer placed between the polished steel top plate and the IRE. The thickness of the spacer was 0.3 mm, and the exposed area of the coated IRE was 40 mm long × 10 mm wide. The total volume of the cell was 120 μL. The liquid flow rate was 1 mL/min in all experiments; as a result, the residence time in the cell was 7.2 s.

The ATR-IR cell was assembled with the coated IRE and mounted in the sample compartment of an infrared spectrometer (Bruker Tensor 27) equipped with a MCT detector. Once the cell was assembled in the IR spectrometer, it was flushed with Ar/H_2O until a stable water spectrum was obtained. Subsequently, the catalyst was reduced *in situ* by introducing H_2/H_2O (4.1×10^{-4} mol/L H_2). This catalyst is designated H–Pd/Al_2O_3, because the Pd/Al_2O_3 catalyst contains hydrogen.

In gas phase, formation of β-palladium-hydride occurs at hydrogen pressures above 0.025 bar [27]. The chemical potential of dissolved hydrogen is equal to that of hydrogen in the gas mixture as hydrogen dissolution is allowed to equilibrate. Thus, exposure of palladium catalysts to water saturated with hydrogen pressure >0.025 bar will also result in the formation of β-palladium-hydride. After reduction in water, the H–Pd/Al_2O_3 catalyst used in this study should contain β-palladium-hydride ($PdH_{0.7}$). Taking the dispersion (45% [24,25]) into account, the maximum hydrogen concentration on the surface and in the palladium is H/Pd = 0.8/1. This number will be used to compare to the amounts of molecules converted. Reduction using lower hydrogen concentration (8.2×10^{-6} mol/L H_2; saturation at 0.01 bar) should result in surface hydrogen and α-palladium-hydride only ($PdH_{0.05}$). The $N_xO_yH_z$ species formed on the catalyst after reduction at low hydrogen concentrations (not presented in this study) are identical to the $N_xO_yH_z$ species shown in the present study with the catalyst reduced at high hydrogen concentrations; only the amounts (observed ATR-IR peak intensities) were lower, because less hydrogen was available.

The ATR-IR spectra were recorded at room temperature (294 K) in an air-conditioned room. Each spectrum was acquired by averaging of 128 scans taken with a resolution of 4 cm^{-1}, which took about 78 s. This was approximately 10 times longer than the liquid residence time in the cell. Thus, each spectrum represents the overall changes in the spectra over a period of about 78 s. The interval between the start of two subsequent spectra was 90 s. As a result, the time resolution between the spectra was 90 s. Shorter data acquisition times led to unacceptably low signal-to-noise ratios.

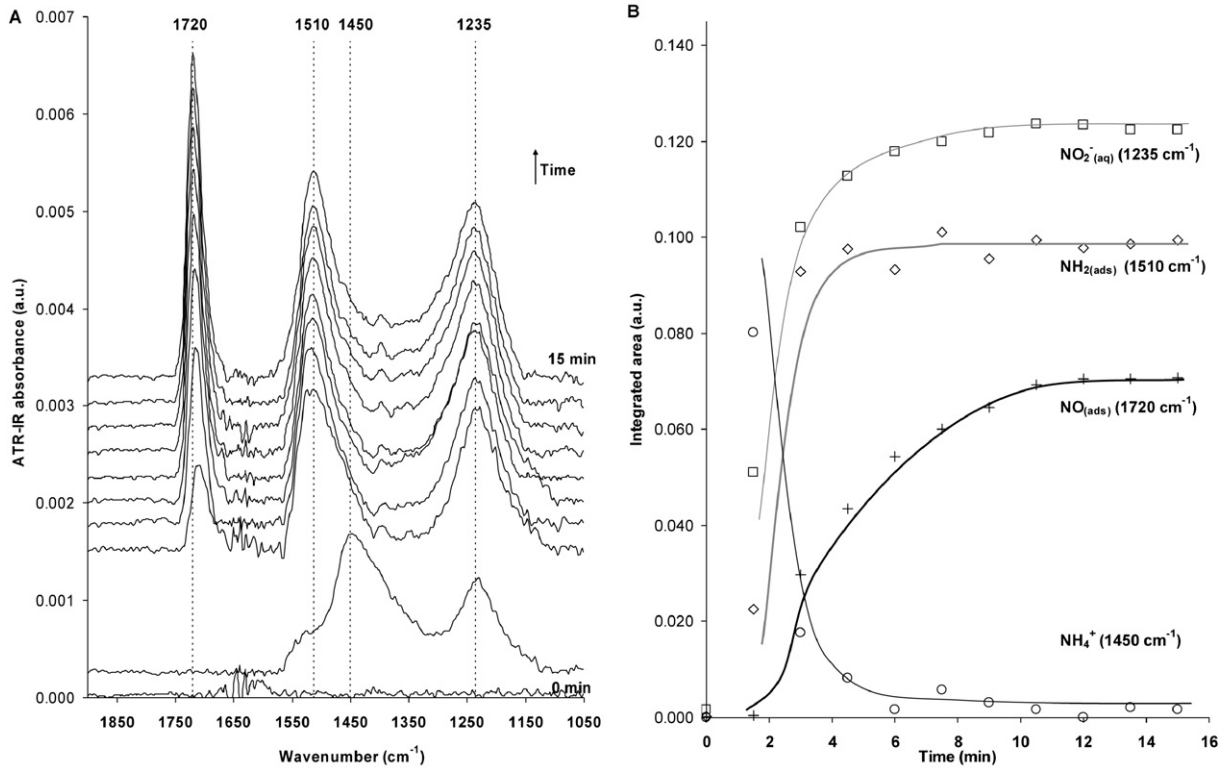

Fig. 2. (A) Water corrected ATR-IR spectra while flowing a solution of $NO^-_{2(aq)}$ (4.3×10^{-4} mol/L) over H–Pd/Al_2O_3 at pH 7.0; (B) integrated peak areas of observed species during $NO^-_{2(aq)}$ flow.

2.3. Data treatment

As recently shown by our group, the ATR-IR spectra must be corrected for the infrared absorbance of water [23]. Details on the subtraction of a scaled background for dissolved gasses are provided in that same report. After subtraction of the water spectra, the residual spectra showed a complexity of peaks. To calculate the integrated peak area of the respective peaks, curve fitting was applied, using a Lorentz function. The applied Lorentz line-shape function centered at the frequency ω_0 is given by:

$$I(\omega) = A \cdot \frac{2}{\pi} \cdot \frac{w}{4 \cdot (\omega - \omega_0) + w^2},$$

where $I(\omega)$ is the intensity at a given frequency ω, A is the integrated area; and w is the full width at half maximum intensity.

3. Results and discussion

3.1. Adsorption of $NO^-_{2(aq)}$ on H–Pd/Al_2O_3

Adsorption of $NO^-_{2(aq)}$ (4.3×10^{-4} mol/L) was performed at pH 7.0 on H–Pd/Al_2O_3; infrared peaks evolved as shown in Fig. 2A. The integrated peak areas during adsorption are shown in Fig. 2B. Initially (i.e., in the first 2 min), infrared peaks evolved at 1450 (width of 62 cm^{-1}) and 1235 cm^{-1}. Subsequently, two other bands developed at 1510 and 1705 cm^{-1}, with the latter shifting to 1720 cm^{-1} with increasing exposure time to $NO^-_{2(aq)}$, as can be seen in Fig. 2A.

$NO^-_{2(aq)}$ was detected at 1235 cm^{-1}, with a peak width of 78 cm^{-1}, which is identical to the peak for $NO^-_{2(aq)}$ in blank experiments published recently by our group [24]. During adsorption of $NO^-_{2(aq)}$ on H–Pd/Al_2O_3, the intensity of the peak for $NO^-_{2(aq)}$ continued to increase slightly with time, possibly due to conversion of NO^-_2 during the first minutes; thus, for some time, the concentration of $NO^-_{2(aq)}$ is lower than that in the feed. No clear peaks for $NO^-_{x(ads)}$ ($x = 2, 3$) on palladium were detected (expected at 1405 and 1325 cm^{-1}), compared with adsorption of $NO^-_{2(aq)}$ on Pd/Al_2O_3 without preadsorbed hydrogen (passivated in air) [24]; however, the possible presence of a small amount of $NO^-_{x(ads)}$ cannot be excluded, due to the increased intensity between 1300 and 1450 cm^{-1}. Nevertheless, the intensity of a possible broad band at that position would be at least one order of magnitude lower compared with that of $NO^-_{x(ads)}$ on a passivated Pd/Al_2O_3 catalyst [24].

According to previous blank experiments with NH^+_4, the band developing initially at 1450 cm^{-1} can be assigned to NH^+_4 [24]. The band at 1510 cm^{-1} was observed during decomposition of hydroxylamine on Pd/Al_2O_3 and was assigned to $NH_{2(ads)}$ [24]. NH^+_4 is either adsorbed on palladium or present in the liquid; no distinction can be made based on the infrared spectrum [24].

The only new (as-yet not assigned) signal was observed at 1705 cm^{-1}, which shifted to 1720 cm^{-1} with increasing time. The observed blue shift is characteristic of molecules with a dipole, such as NO. To the best of our knowledge, only one

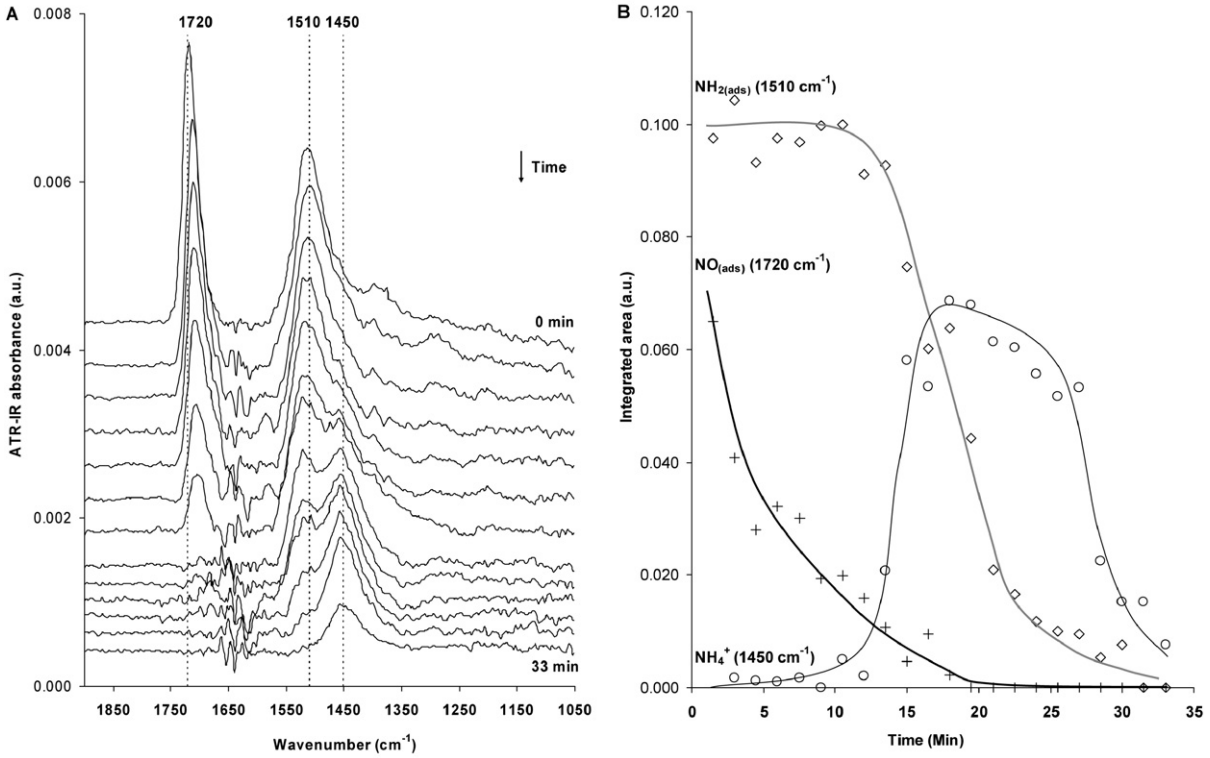

Fig. 3. (A) Water corrected ATR-IR spectra while H_2/H_2O (4.1×10^{-6} mol/L H_2) was flown over Pd/Al_2O_3 with $NO_{(ads)}$ and $NH_{2(ads)}$, previously formed during adsorption of $NO^-_{2(aq)}$ on H–Pd/Al_2O_3 (Fig. 2); (B) integrated peak areas during flow of H_2/H_2O.

paper has reported NO adsorption on palladium in water, examined with IR spectroscopy [28]. In that study, adsorbed NO on a Pd(111) electrode, held at a potential of 0.4 V, was detected by a single peak that blue-shifted from 1720 to 1748 cm^{-1} with increasing coverage [28].

The formation of adsorbed NO during heterogeneous hydrogenation of nitrite over supported noble metal catalysts has been proposed in the literature but not supported by experimental evidence [5,6,10,11]. In electrochemistry, on the other hand, NO adlayers were prepared from nitrate and nitrite solutions on platinum electrodes [29–31], thereby demonstrating formation of adsorbed NO as an intermediate during the electrochemical reduction of nitrite on platinum electrodes. Consequently, based on the literature and the observed blue shift, we assign the infrared peak at 1705–1720 cm^{-1} to NO adsorbed on palladium. Unfortunately, direct experimental confirmation via adsorption of NO from water is not possible, because NO dissolved in water is not stable.

Initially, the peak for NH_4^+ dominates the spectrum; in addition to NH_4^+, a small shoulder indicating the formation of $NH_{2(ads)}$ can already be seen in the spectrum recorded after 90 s of adsorption in Fig. 2A. Formation of NH_4^+ on the palladium surface during the initial adsorption of $NO^-_{2(aq)}$ can occur via reaction with hydrogen on the H–Pd/Al_2O_3 catalyst. Formation of NH_4^+ at high hydrogen concentrations is in good agreement with reports on the heterogeneous hydrogenation of NO_2^- in batch reactors over palladium catalysts. The selectivity to NH_4^+ has been found to increase with increasing hydrogen concentration [4,8,32,33]. Fig. 2B clearly shows that the NH_4^+ signal is initially high but subsequently decreases, whereas the signals for both $NH_{2(ads)}$ and $NO^-_{2(aq)}$ gain intensity during the subsequent 4–6 min. Clearly, the signal of $NH_{2(ads)}$ stabilizes earlier than that of $NO^-_{2(aq)}$; moreover, the formation of $NO_{(ads)}$ is delayed and stabilizes no earlier than after 12 min of reaction, along with the $NO^-_{2(aq)}$ signal. Because no hydrogen is added during the adsorption of nitrite, NH_4^+ and $NH_{2(ads)}$ species must be formed from hydrogen on or in the catalyst. It can be estimated that just a 2.5 min nitrite flow would be required to convert all hydrogen present on or in the catalyst into NH_4^+, assuming an H/Pd ratio of 0.8 (maximum amount of hydrogen possibly present in the palladium particles, as described in Section 2, *vide ante*) and assuming complete conversion of nitrite. This is in reasonable agreement with the fact that the initial intensity of NH_4^+ is high, then drops close to zero after 4 min, as well as with the fact that the NH_2 intensity stabilizes in the same time window. Subsequently, NO is formed that seems to originate from NO_2^-, similar to the preparation of NO adlayers on platinum electrodes in electrochemistry [29–31].

3.2. *Hydrogenation of $NO_{(ads)}$ and $NH_{2(ads)}$ on H–Pd/Al_2O_3*

After the adsorption of $NO^-_{2(aq)}$ on H–Pd/Al_2O_3, as shown in Fig. 2, the cell was flushed with Ar/H_2O. During flushing, all adsorbed species appeared stable, whereas $NO^-_{2(aq)}$ (1235 cm^{-1}) was flushed out of the cell, resulting in the top spectrum in Fig. 3. Subsequently, H_2/H_2O (4.1×10^{-6} mol/L H_2) was introduced into the cell, after which infrared peaks evolved, as shown in Fig. 3. Experiments were performed at

very low hydrogen concentrations to slow the reaction rates (4.1×10^{-6} mol/L H_2, saturated at 0.001 bar H_2).

First, the peak at 1720 cm^{-1} ($NO_{(ads)}$) decreased in intensity during exposure to hydrogen while simultaneously shifting to 1705 cm^{-1}. Initially, no changes in intensity of the peaks at 1510 cm^{-1} ($NH_{2(ads)}$) and 1450 cm^{-1} (NH_4^+) were observed (Figs. 3A and 3B). It took about 12 min (Fig. 3B) for the peak for $NH_{2(ads)}$ at 1510 cm^{-1} to begin to decrease and for a band for NH_4^+ to appear at 1450 cm^{-1}. The NH_4^+ band reached a maximum after 20 min and subsequently decreased to almost zero after 35 min.

During the initial hydrogenation of adsorbed NO and NH_2 (Fig. 3), a clear decrease in peak intensity was observed for $NO_{(ads)}$, whereas no change in $NH_{2(ads)}$ or NH_4^+ was detected for the first 12 min. Consequently, the hydrogenation product of $NO_{(ads)}$ was neither $NH_{2(ads)}$ nor NH_4^+. $NO_{(ads)}$ must be either desorbed or converted into a product that cannot be detected by ATR-IR. So far, NO has not been detected in the gas phase or aqueous phase during hydrogenation of nitrite [5,8]. Furthermore, because NO adsorbs more strongly on palladium than hydrogen, we suggest that in the present experiment, $NO_{(ads)}$ was hydrogenated to N_2, which obviously cannot be observed by IR spectroscopy. We are currently developing a method for detecting very small amounts of dissolved gases in aqueous solutions, to unambiguously determine the hydrogenation product of $NO_{(ads)}$ [34].

The fact that $NH_{2(ads)}$ decreases simultaneously while NH_4^+ is increasing points strongly to the hydrogenation of $NH_{2(ads)}$ to NH_4^+ in the presence of hydrogen. Initially, the rate of NH_4^+ formation from $NH_{2(ads)}$ is high, because much $NH_{2(ads)}$ is available. After some time, the surface becomes depleted in $NH_{2(ads)}$; because NH_4^+ is flushed out of the cell continuously, this results in a decreased intensity of the NH_4^+ band.

During the first 12 min of hydrogenation of adsorbed NO and NH_2 (Fig. 3) only $NO_{(ads)}$ was converted; $NH_{2(ads)}$ was converted later. The maximal initial surface coverage of $NO_{(ads)}$ and $NH_{2(ads)}$ can be estimated, assuming complete consumption of the hydrogen present in the water entering the reactor. Based on the equations of both surface reactions,

$$2NO_{(ads)} + 2H_2 \rightarrow N_2 + 2H_2O$$

and

$$2NH_{2(ads)} + H_2 + 2H_2O \rightarrow 2NH_4^+ + 2OH^-,$$

it follows that a maximum of 4.9×10^{-8} mol $NO_{(ads)}$ was converted within the first 12 min, corresponding to an initial NO coverage of 4% at maximum. The actual coverage may have been even lower, because part of the H_2 might not have interacted with the catalyst film due to bypassing. In the subsequent 20 min, $NH_{2(ads)}$ was converted into NH_4^+, corresponding to a maximal initial NH_2 coverage of 6%. These calculations also explain the high NH_4^+ signal shown in Fig. 2. If the adsorption of nitrite on H–Pd/Al_2O_3 resulted in the mentioned coverage of $NO_{(ads)}$ and $NH_{2(ads)}$, this means that only 20% of the initially present amount of hydrogen was consumed. The remaining 80% hydrogen must have been consumed during the initial formation of NH_4^+, as reflected in the high initial peak intensity for NH_4^+ shown in Fig. 2.

Although the final NO coverage was as low as 4% (Fig. 2), a clear blue shift, due to dipole–dipole coupling, was observed with increasing NO coverage during the adsorption of nitrite on H–Pd/Al_2O_3. Blue shifts for NO have indeed been reported at an NO coverage as low as 2% [35], demonstrating consistency of the experimental observations in the present study on the blue shift of the peak for $NO_{(ads)}$ with increasing NO coverage.

Interestingly, no adsorbed nitrite was detected after exposure of H–Pd/Al_2O_3 to a nitrite solution (Fig. 2). Because the maximal coverage of NO and NH_2 is only 10%, a sufficient number of sites for nitrite adsorption should be available. We have shown recently that nitrite adsorbs on a palladium surface covered by oxygen [24]. From the present experiments, it can be concluded that nitrite reacts with adsorbed hydrogen on the palladium particles supposedly via an Eley–Rideal mechanism, leaving an empty Pd surface on which nitrite does not adsorb. In addition, nitrite adsorption has been reported to be structure-sensitive in the electrochemical reduction of nitrite and nitrate over platinum electrodes [36–38]. A finding that the NO and NH_2 produced covered the specific palladium sites that can adsorb nitrite (unlike the situation in the present study) would also explain the fact that no adsorbed nitrite was detected (Fig. 2).

The result shown in Fig. 3 demonstrates that $NO_{(ads)}$ was much more reactive toward hydrogen than $NH_{2(ads)}$, because hydrogenation of $NH_{2(ads)}$ occurred after almost all of the $NO_{(ads)}$ disappeared. This observation is qualitatively in agreement with the fact that Pd catalysts generally exhibit high selectivity to nitrogen.

3.3. Continuous hydrogenation of $NO_{2(aq)}^-$ over H–Pd/Al_2O_3

To examine the *in situ* nitrite hydrogenation over Pd/Al_2O_3, a solution containing 4.3×10^{-4} mol/L $NO_{2(aq)}^-$ and 4.1×10^{-4} mol/L H_2 was introduced to the cell with a prereduced H–Pd/Al_2O_3 catalyst layer (Fig. 4). One clear peak at 1235 cm^{-1} with a width of 79 cm^{-1} was detected, which is assigned to $NO_{2(aq)}^-$ [24]. In addition, an increase in intensity was observed between 1550 and 1300 cm^{-1}, indicating the presence of adsorbed species at low coverage. But the low intensity did not allow identification of the individual adsorbed species. Based on kinetic data on nitrite hydrogenation [39], the conversion of $NO_{2(aq)}^-$ is estimated as <1% under our experimental conditions. The low surface coverage of the hydrogenation intermediates found here is most likely due to the rapid subsequent hydrogenation of the surface intermediates.

Because no adsorbed species were detected during continuous hydrogenation using a H_2/NO_2^- ratio of 1, solutions with lower hydrogen concentrations were applied. This slowed down the reaction rates and increased the likelihood of detecting reaction intermediates *in situ*. It turned out that hydrogenation intermediates and products were observed only at hydrogen concentrations $\leqslant 2.1 \times 10^{-5}$ mol/L. *In situ* ATR-IR spectra during hydrogenation of 4.3×10^{-4} mol/L $NO_{2(aq)}^-$ using different hydrogen concentrations are shown in Figs. 5A, 5C, and 5E

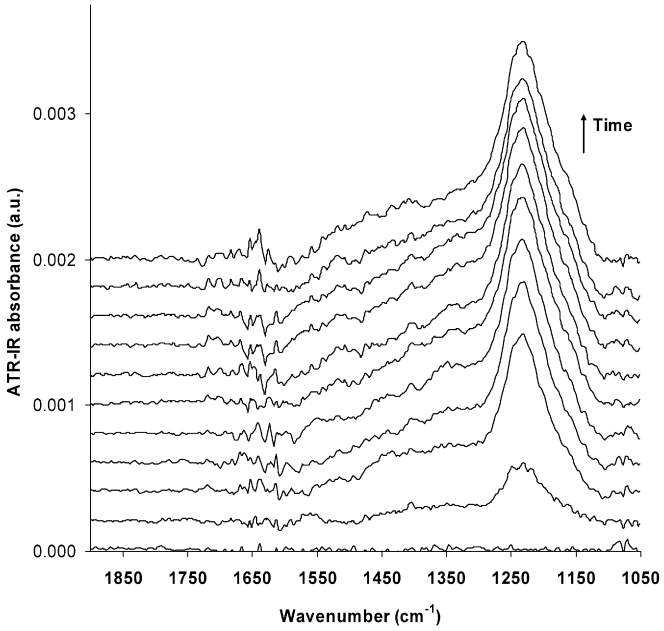

Fig. 4. Water corrected ATR-IR spectra during hydrogenation of $NO_{2(aq)}^-$ over H–Pd/Al_2O_3 (4.3×10^{-4} mol/L $NO_{2(aq)}^-$ and 4.1×10^{-4} mol/L H_2) (the time between spectra was 1.5 min).

along with the integrated peak areas shown in Figs. 5B, 5D, and 5F.

Fig. 5 shows that surface intermediates resulting from the reaction between nitrite and hydrogen was observed at the three hydrogen concentrations applied. Within 15 min, clear infrared peaks evolved at 1705–1715, 1510, 1450, and 1235 cm^{-1}; which are assigned to $NO_{(ads)}$, $NH_{2(ads)}$, NH_4^+, and $NO_{2(aq)}^-$, respectively. In addition, a shoulder appeared at around 1575–1550 cm^{-1} that has not yet been assigned. The nature of this species remains unknown. Because bridged adsorbed NO is normally detected at lower frequencies than linear adsorbed NO (see [24] and references therein), it can be speculated that the shoulder represents NO adsorbed on palladium in bridged geometry.

No significant amount of adsorbed NO_2^- on palladium was detected (1405 and 1325 cm^{-1}), whereas $NO_{2(aq)}^-$ was observed at 1235 cm^{-1}. Moreover, no differences in the intensity of the peak for $NO_{2(aq)}^-$ was observed at the hydrogen pressures applied, which agrees with our claim of low $NO_{2(aq)}^-$ conversion, as discussed earlier. In fact, the $NO_{2(aq)}^-$ intensities in Figs. 5 and 4 were similar. Moreover, the hydrogen conversion can be estimated as 1–6% based on kinetic data [39], demonstrating that the catalyst certainly was not exhausted in hydrogen during hydrogenation.

The development of the other bands with time (Figs. 5B, 5D and 5F) illustrates that in all cases, NH_4^+ was initially formed on the palladium surface while (as for the titration experiments) $NO_{2(aq)}^-$ also was observed (Fig. 2). The bands of $NO_{(ads)}$ and $NH_{2(ads)}$ increased in intensity after approximately 3 min, when the NH_4^+ signal began to decrease in intensity. This delay is similar to that seen when nitrite was flowed only over H–Pd/Al_2O_3 (Fig. 2) and can be explained by the time needed to introduce a sufficient amount of nitrite to convert the excess of adsorbed hydrogen on the prereduced H–Pd/Al_2O_3 catalyst (*vide ante*). Thus, the first 10 min of all of the experiments presented in Fig. 5 represent the same transient response as shown in Fig. 2. Only after 10 min, when stable levels were observed, was steady-state hydrogenation achieved.

It also is evident that larger amounts of the surface intermediates $NO_{(ads)}$, $NH_{2(ads)}$, and NH_4^+ were observed at lower hydrogen concentrations. Clearly, decreasing the H_2/NO_2^- ratio slowed the hydrogenation of the intermediates, thereby resulting in increased concentrations of the surface intermediates. Moreover, the ratios of the amounts of the respective surface intermediates varied with the hydrogen concentration, as shown in Fig. 6.

The ratio between the integrated peak intensities of $NO_{(ads)}$ and $NH_{2(ads)}$ at steady state (after 15 min time on stream) decreased with increasing hydrogen concentration. Moreover, the $NH_{2(ads)}/NH_4^+$ ratio remained constant in all cases. In the previous section, it was shown that $NH_{2(ads)}$ is converted to NH_4^+, whereas $NO_{(ads)}$ most likely is converted to N_2. Consequently, the decreased $NO_{(ads)}/NH_{2(ads)}$ ratio indicates a higher selectivity to NH_4^+ with increasing hydrogen concentration. This explains the increased selectivity to NH_4^+ with increasing hydrogen pressure as reported for the hydrogenation of nitrite in conventional batch reactors [4,9,32,33].

3.4. Nitrite hydrogenation mechanism

This paper provides some detailed insight into the surface intermediates and, consequently, the mechanism of the heterogeneous catalytic hydrogenation of nitrite in water over Pd/Al_2O_3 as obtained by *in situ* ATR-IR spectroscopy. The adsorption of $NO_{2(aq)}^-$ on H–Pd/Al_2O_3 yields $NO_{(ads)}$, $NH_{2(ads)}$ and NH_4^+. These species originate from reaction with hydrogen on the palladium surface (Figs. 2 and 5). Moreover, subsequent hydrogenation showed that $NO_{(ads)}$ most likely is converted into N_2, whereas the hydrogenation of $NH_{2(ads)}$ yields only NH_4^+. Interestingly, the production of NH_4^+ begins only after most of the $NO_{(ads)}$ has disappeared (Fig. 3). Our findings clearly demonstrate that NH_4^+ and nitrogen are formed via two parallel stepwise hydrogenation processes, as shown in Scheme 1. Moreover, these two reactions pathways are independent. The observation that $NH_{2(ads)}$ cannot be hydrogenated to N_2 is obvious; the observation that $NO_{(ads)}$ cannot be converted to $NH_{2(ads)}$ or NH_4^+ is unexpected; this is indicated by the interrupted arrow in Scheme 1.

In Scheme 1, the actual observed species are highlighted with a box. Clearly, the hydrogenation of nitrite to $NH_{2(ads)}$ must be a sequence of elementary reaction steps. Because $NO_{(ads)}$ evidently is not an intermediate for NH_4^+ formation (Fig. 3), there must be a reaction pathway from NO_2^- to NH_4^+, excluding $NO_{(ads)}$ as an intermediate species. The most feasible reaction path is the addition of hydrogen to nitrite as the first step to form HNO_2^-, which undergoes further stepwise hydrogenation to $NH_{2(ads)}$. Formation of HNO_2^- as an

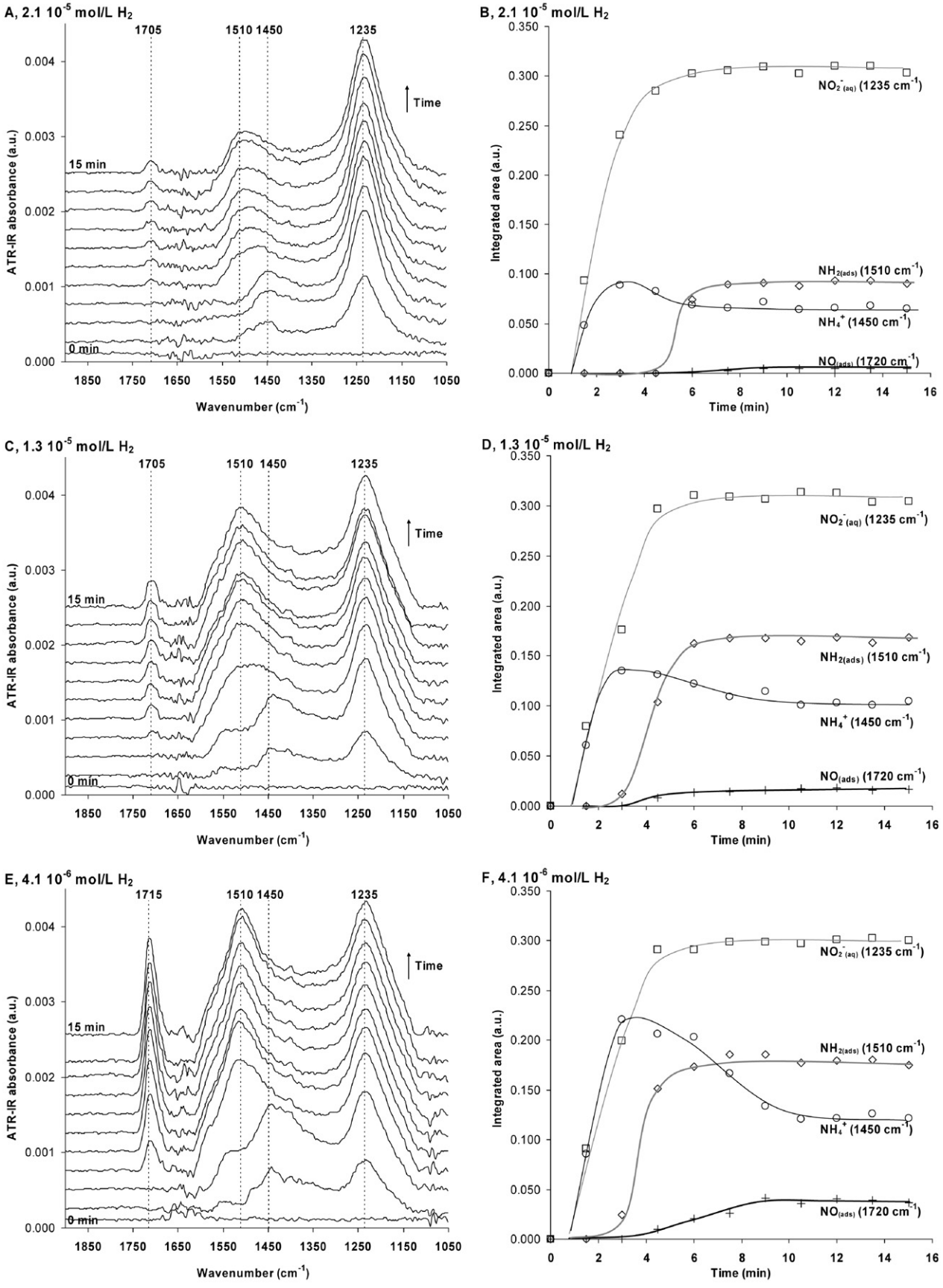

Fig. 5. (A, C, E) Water corrected ATR-IR spectra during hydrogenation of $NO_{2(aq)}^{-}$ (4.3×10^{-4} mol/L) over H–Pd/Al_2O_3 and (B, D, E) integrated peak areas during hydrogenation ((A and B) 2.1×10^{-5} mol/L H_2, (C and D) 1.3×10^{-5} mol/L H_2, (E and F) 4.1×10^{-6} mol/L H_2).

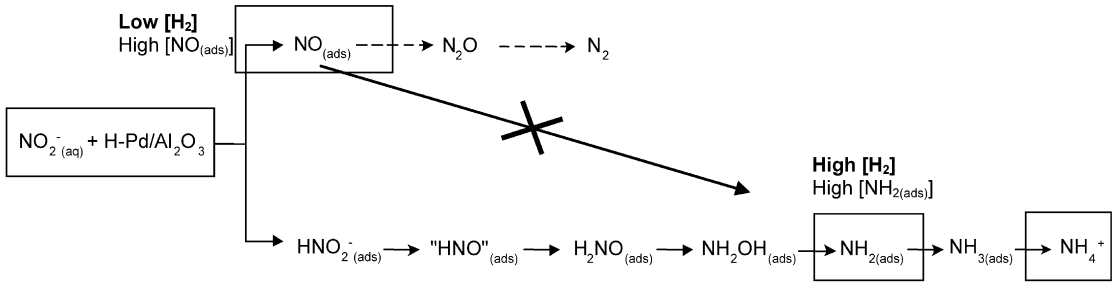

Scheme 1. Improved reaction scheme of the catalytic hydrogenation of nitrite over Pd/Al_2O_3. The reactions in the boxes are based on the findings in the present paper. The other reactions in the scheme have been discussed before in literature [53]. The dotted lines represent possible reaction pathways for N_2O and N_2 formation, although at present there is no evidence for these pathways.

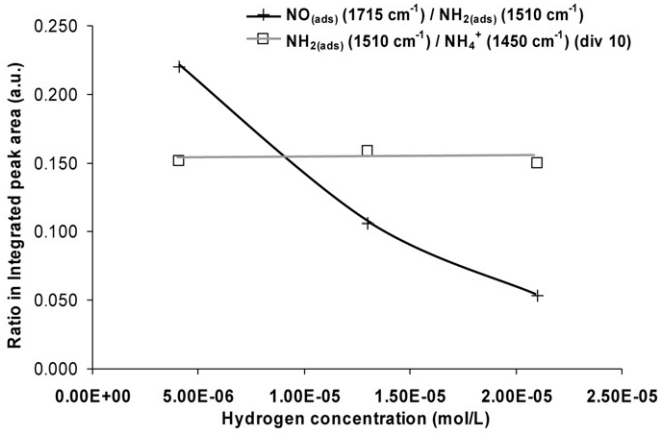

Fig. 6. Ratio between the peak intensity of $NO_{(ads)}$ and $NH_{2(ads)}$ and between $NH_{2(ads)}$ and NH_4^+ at steady state during continuous hydrogenation at varying hydrogen concentrations.

intermediate for the electrochemical reduction of nitrite over platinum has been suggested in the literature [37,40–42]. In addition, the formation of NH_4^+ via hydrogenation of $HNO^-_{2(ads)}$ is supported by the reaction mechanisms proposed from the electrochemical reduction of nitrate and nitrite over platinum electrodes [36,40–43]. Dissociation of hydrogen is assumed to be the first step, followed by reaction with nitrite [11–14]. Unfortunately, the present study provides no clear evidence for the presence of $HNO^-_{2(ads)}$ (expected at wave numbers around 1260–1280 cm^{-1}); however, its presence cannot be excluded, because the signal could be easily masked by the large peak at 1235 cm^{-1}. $NH_{2(ads)}$ was observed only during adsorption of $NO^-_{2(aq)}$ on H–Pd/Al_2O_3 (Fig. 2), suggesting that the entire stepwise hydrogenation process starting from NO_2^- proceeds much faster than subsequent hydrogenation of $NH_{2(ads)}$ into NH_4^+. In addition, NH_2OH is considered a likely intermediate during the formation of NH_4^+ (Scheme 1), because we have recently shown that the $NH_{2(ads)}$ intermediate also arises from decomposition and/or reaction of NH_2OH on Pd/Al_2O_3 [24].

The formation of nitrogen, on the other hand, must proceed via $NO_{(ads)}$ as an intermediate. From the present study, it is clear that $NO_{(ads)}$ is formed on the palladium surface during the hydrogenation of nitrite, in agreement with proposed mechanisms based on kinetic studies [5,6,10,11]. At present, the mechanism of N_2 formation is unclear, but the most frequently suggested mechanism involves dimerization of $NO_{(ads)}$ [43–52] with N_2O as an intermediate; this was not observed in the present study, however, possibly due to the rapid reduction of N_2O to N_2 reported previously for palladium catalysts [50].

The proposed scheme with two parallel reaction pathways for NH_4^+ and nitrogen contradicts reaction schemes for the heterogeneous hydrogenation of nitrite over supported noble metal catalysts proposed in the literature. Adsorbed NO has been proposed as an intermediate in the formation of both nitrogen and NH_4^+ [5,6,10,11]. In our improved reaction scheme, adsorbed NO is an intermediate, but it hydrogenates only to N_2, whereas $NH_{2(ads)}$ is converted to NH_4^+ via $HNO^-_{2(ads)}$ as an intermediate. The fact that $NO_{(ads)}$ is apparently much more reactive than $NH_{2(ads)}$ means that reasonable selectivity to N_2 is within reach for Pd catalysts. Moreover, our experiments demonstrate that the concentrations of $NO_{(ads)}$ and $NH_{2(ads)}$ are affected by the hydrogen concentration; at high hydrogen concentration, the $NH_{2(ads)}$ concentration increased compared with the surface coverage of $NO_{(ads)}$. This explains qualitatively that selectivity to N_2 decreases with increasing H_2 pressure, as has been reported previously [4,8,33].

4. Conclusion

This study investigated the relevant surface intermediates in the catalytic hydrogenation of NO_2^- over Pd/Al_2O_3 in water. Adsorbed NO, NH_2, and NH_4^+ are detected as surface intermediates on the palladium surface during reaction of $NO^-_{2(aq)}$ with surface hydrogen. $NO_{(ads)}$ is more reactive toward hydrogen than $NH_{2(ads)}$, and hydrogenation of $NH_{2(ads)}$ is the rate determining step in the reaction sequence to NH_4^+. Hydrogenation of adsorbed NO on palladium results in the formation of a reaction product that is not IR-active (most likely nitrogen), whereas no NH_4^+ is formed. NH_4^+, on the other hand, is formed solely via hydrogenation of the $NH_{2(ads)}$ intermediate. Our findings clearly demonstrate that the formation of nitrogen and NH_4^+ proceeds via two independent pathways. Consequently, we have proposed a revised reaction scheme. Increasing selectivity to NH_4^+ with increasing hydrogen concentration is in good agreement with preferential formation of $NH_{2(ads)}$ over $NO_{(ads)}$ at high hydrogen concentrations.

Acknowledgments

This work was supported by DSM Research and performed under the auspices of the Dutch Institute for Research in Catalysis (NIOK). The authors thank Dr. Henk Oevering for the valuable discussions and Mr. Bert Geerdink for technical support.

References

[1] World Health Organization, Water and Health in Europe, WHO, Regional Office for Europe, Copenhagen, 2002.
[2] A. Kapoor, T. Viraraghavan, J. Environ. Eng. 123 (1997) 371.
[3] K.D. Vorlop, T. Tacke, Chem. Ing. Tech. 61 (1989) 836.
[4] S. Hörold, K.D. Vorlop, T. Tacke, M. Sell, Catal. Today 17 (1993) 21.
[5] S. Hörold, T. Tacke, K.D. Vorlop, Environ. Technol. 14 (1993) 931.
[6] K.D. Vorlop, U. Prusse, Environ. Catal. (1999) 195.
[7] M. Hahnlein, U. Prusse, J. Daum, V. Morawsky, M. Koger, M. Schroder, M. Schnabel, K.D. Vorlop, Prep. Catal. VII (1998) 99.
[8] U. Prüsse, J. Daum, C. Bock, K.D. Vorlop, Stud. Surf. Sci. Catal. 130 (2000) 2237.
[9] A. Pintar, J. Batista, J. Levec, Water Sci. Technol. 37 (1998) 177.
[10] J. Wärnå, I. Turunen, T. Salmi, T. Maunula, Chem. Eng. Sci. 49 (1994) 5763.
[11] A. Pintar, J. Batista, J. Levec, T. Kijiuchi, Appl. Catal. B 11 (1996) 81.
[12] U. Prüsse, M. Hahnlein, J. Daum, K.D. Vorlop, Catal. Today 55 (2000) 79.
[13] K. Daub, G. Emig, M.J. Chollier, M. Callant, R. Dittmeyer, Chem. Eng. Sci. 54 (1999) 1577.
[14] J. Daum, K.D. Vorlop, Chem. Eng. Technol. 22 (1999) 199.
[15] N.J. Harrick, Internal Reflection Spectroscopy, Interscience, New York, 1967.
[16] T. Bürgi, A. Baiker, J. Phys. Chem. B 106 (2002) 10649.
[17] S.D. Ebbesen, B.L. Mojet, L. Lefferts, J. Catal. 246 (2007) 66.
[18] R. He, R.R. Davda, J.A. Dumesic, J. Phys. Chem. B 109 (2005) 2810.
[19] N. Kizhakevariam, X. Jiang, M.J. Weaver, J. Chem. Phys. 100 (1994) 6750.
[20] I. Ortiz-Hernandez, C.T. Williams, Langmuir 19 (2003) 2956.
[21] N.C. Yee, G.S. Chottiner, D.A. Scherson, J. Phys. Chem. B 109 (2005) 7610.
[22] T. Bürgi, A. Baiker, Adv. Catal. 50 (2006) 227.
[23] S.D. Ebbesen, B.L. Mojet, L. Lefferts, Langmuir 22 (2006) 1079.
[24] S.D. Ebbesen, B.L. Mojet, L. Lefferts, Langmuir 24 (2008) 869.
[25] S.D. Ebbesen, Spectroscopy under the surface—In situ ATR-IR studies of heterogeneous catalysis in water, Doctoral thesis, Gildeprint B.V., Enschede, 2007.
[26] R.C. Weast (Ed.), Handbook of Chemistry and Physics, 48th ed., The Chemical Rubber Co., Cleveland, OH, 1970.
[27] F.A. Lewis, The Palladium Hydrogen System, Academic Press, New York, 1967.
[28] S. Zou, R. Gomez, M.J. Weaver, J. Electroanal. Chem. 474 (1999) 155.
[29] A. Rodes, R. Gomez, J.M. Perez, J.M. Feliu, A. Aldaz, Electrochim. Acta 41 (1996) 729.
[30] V. Rosca, G.L. Beltramo, M.T.M. Koper, Langmuir 21 (2005) 1448.
[31] E. Casero, C. Alonso, J.A. Martin-Gago, F. Borgatti, R. Felici, F. Renner, T.L. Lee, J. Zegenhagen, Surf. Sci. 507–510 (2002) 688.
[32] Y. Matatov-Meytal, V. Barelko, I. Yuranov, M. Sheintuch, Appl. Catal. B 27 (2000) 127.
[33] Y. Matatov-Meytal, Y. Shindler, M. Sheintuch, Appl. Catal. B 45 (2003) 127.
[34] D. Radivojevic, K. Seshan, L. Lefferts, J. Catal. (2008), submitted for publication.
[35] B.E. Hayden, Surf. Sci. 131 (1983) 419.
[36] G.E. Dima, G.L. Beltramo, M.T.M. Koper, Electrochim. Acta 50 (2005) 4318.
[37] S. Ye, H. Kita, J. Electroanal. Chem. 346 (1993) 489.
[38] J.F.E. Gootzen, R.M. van Hardeveld, W. Visscher, R.A. van Santen, J.A.R. van Veen, Recl. Trav. Chim. Pays-Bas 15 (1996) 480.
[39] A. Pintar, G. Bercic, AIChE J. 44 (1998) 2280.
[40] K. Nishimura, K. Machida, M. Enyo, Electrochim. Acta 36 (1991) 877.
[41] F. Balbaud, G. Sanchez, G. Santarini, G. Picard, Eur. J. Inorg. Chem. 4 (2000) 665.
[42] A. Rodes, R. Gomez, J.M. Orts, J.M. Feliu, A. Aldaz, J. Electroanal. Chem. 359 (1993) 315.
[43] M.C.P.M. da Cunha, J.P.I. De Souza, F.C. Nart, Langmuir 16 (2000) 771.
[44] L.J.J. Janssen, M.M.J. Pieterse, E. Barendrecht, Electrochim. Acta 22 (1977) 27.
[45] I. Paseka, J. Vonkova, Electrochim. Acta 25 (1980) 1251.
[46] I. Paseka, A. Hodinar, Electrochim. Acta 27 (1982) 1461.
[47] J.A. Colucci, M.J. Foral, S.H. Langer, Electrochim. Acta 30 (1985) 521.
[48] A.C.A. de Vooys, M.T.M. Koper, R.A. van Santen, J.A.R. van Veen, Electrochim. Acta 46 (2001) 923.
[49] A.C.A. de Vooys, G.L. Beltramo, B. van Riet, J.A.R. van Veen, M.T.M. Koper, Electrochim. Acta 49 (2004) 1307.
[50] A.C.A. de Vooys, M.T.M. Koper, R.A. van Santen, J.A.R. van Veen, J. Catal. 202 (2001) 387.
[51] R.R. Gadde, S. Bruckenstein, J. Electroanal. Chem. 50 (1974) 163.
[52] D.D. De, J.D. Englehardt, E.E. Kalu, J. Electrochem. Soc. 147 (2000) 4573.
[53] V. Rosca, M.T.M. Koper, Surf. Sci. 584 (2005) 258.